Advances in Machinery, Materials Science and Engineering Application
M. Chen et al. (Eds.)

doi:10.3233/ATDE220438

Study on Preparation and Reaction Mechanism of B_4C/β-Sialon/SiC/Al_2O_3 Composite Powder

Hao YANG [a], Chengji DENG [a], Chao YU [a], Jun DING [a,1], Hongxi ZHU [a] and Xiangcheng LI [a,2]
[a] *The State Key Laboratory of Refractories and Metallurgy, Wuhan University of Science and Technology, Wuhan 430081, Hubei, China*

Abstract. B_4C, Si, Al, and γ-Al_2O_3 were used as raw materials, formed β-Sialon and SiC in situ by solid-state reaction for preparation of B_4C composite powder. β-Sialon and SiC grains are uniformly and dispersedly distributed in the composite powder. The effects of the molar ratio of raw materials, nitridation temperature and soaking time for the phase composition, and microstructure of the composite powder were studied. When the molar ratio of B_4C and Si is 2: 3, the composite powder with columnar β-Sialon grains growing alternately can be prepared after nitridation at 1500 °C for 4 h. The liquid phase formed by the melting of Si at high temperature promoted the dissolution of B_4C and the formation of SiC. When the nitridation temperature was increased or the soaking time was prolonged, the gas phase volatilization of Si and Al was intensified, SiC and AlN whiskers tend to be formed in the composite powder.

Keywords. Boron carbide, β-sialon, composite powder

1. Introduction

Boron carbide (B_4C) is an artificial material with a hardness second only to diamond and c-BN [1]. Compared with diamond and c-BN, B_4C powder is usually prepared by a low-cost carbothermal reduction [2,3]. In addition, the B_4C has excellent characteristics such as high melting points, high elastic modulus, low density, and good chemical stability [4]. It is widely used in the fields of grinding processing [5], catalytic carriers [6], and antioxidants of refractory materials [7]. However, the sintering of pure B_4C powder is very difficult because of the high content of covalent bonds of B_4C, which reduces the performance of the material [8].

The preparation of composites helps to give full play to the advantages of multi-component materials [9]. In order to improve the sintering property of B_4C, sintering additives such as metals [10], metal oxides [11], transition metal borides [12], and carbides [13] are often introduced to improve the density of point defects or

[1] Jun Ding, Corresponding author, The State Key Laboratory of Refractories and Metallurgy, Wuhan University of Science and Technology, Wuhan 430081, Hubei, China; E-mail: dingjun@wust.edu.cn.

[2] Xiangcheng Li, Corresponding author, The State Key Laboratory of Refractories and Metallurgy, Wuhan University of Science and Technology, Wuhan 430081, Hubei, China; E-mail: lixiangcheng@wust.edu.cn.

dislocations, so as to achieve the activation effect on grain boundary and volume diffusion and increase the diffusion driving force in the sintering process [14,15]. Yavas et al. [16] prepared B_4C-CNT composite ceramic containing 3 wt.% CNT by SPS sintering, with hardness of 32.8 GPa and fracture toughness of 5.9 $MPa \cdot m^{1/2}$. Liu et al. [17] when the amount of TiB_2 was 20 mol.%, the relative density of B_4C-TiB_2 composite ceramic reached 97.91%, Vickers hardness reached 29.82 GPa, and fracture toughness reached 3.70 $MPa \cdot m^{1/2}$ at 1950 ℃ and 50 MPa by SPS sintering.

The preparation of high-performance composite powder is the basis of subsequent ceramic sintering. For example, the surface modification of powder is an effective means to improve the performance of powder [18-21]. As a reinforcing phase often introduced into composite ceramics, Sialon is a solid solution obtained by partially replacing Si and N atoms in Si_3N_4 with Al and O atoms of Al_2O_3. Still, Sialon is easier to sinter and reach its theoretical density than Si_3N_4. β-Sialon has the best thermal stability and toughness among the four crystal forms of the Sialon phase. Its columnar grains may have a pinning effect at the boron carbide grain boundary, effectively inhibiting grain growth [22,23]. The research shows that the nitridation temperature can significantly affect the grain morphology of the product formed by Si powder and determine the performance of the material [24]. To improve the sintering property of boron carbide ceramics and prepare high-performance boron carbide ceramic materials more efficiently. In this work, boron carbide powders were formed in situ by the solid-phase synthesis reaction of β-Sialon. Through the in-situ nitridation reaction of Si, Al_2O_3 and Al, the β-Sialon is introduced uniformly and dispersedly into the boron carbide. It is expected to play an influential role in promoting sintering and strengthening in the subsequent ceramic sintering.

2. Experiment and Characterization

2.1. Raw Materials and Process

The raw materials include B_4C powder, d_{50}=4.2 μm, Purity ≥ 99.95, Zhongmai Metal Material Co., Ltd. Al powder, analytically pure, Tianjin Kermel Chemical Reagent Co., Ltd. Si powder, d_{50}=1 μm, Shanghai ST-NANO science and technology Co., Ltd. γ-Al_2O_3, purity ≥ 99%, Shanghai Yuanjiang Chemical Co., Ltd.

The chemical formula of β-Sialon is $Si_{6-z}Al_zO_zN_{8-z}$. In this experiment, ingredients were added according to the following chemical Eq. 1.

$$3Si + Al + Al_2O_3 + \frac{5}{2}N_2 = Si_3Al_3O_3N_5 \quad (1)$$

According to the molar ratio of 2:1, 1:1, 2:3, 1:2 of B_4C/Si, they are divided into A1, A2, A3 and A4. Adding Al and γ-Al_2O_3 to mixed in proportion, agate balls and the appropriate amount of ethanol were added according to the material and ball ratio of 1: 3. Grinding and wet mix at the speed of 300 $r \cdot min^{-1}$ for 10 h, and then dry the ground mixture in bake oven at 90 ℃ for 12 h. The dried powder was sieved through a 200 mesh sieve and pressed into powder to a cylindrical sample of Φ10 mm under 4 MPa. Place the samples in a rectangular corundum crucible, using a tubular furnace to maintain a heating rate of 5 ℃/min in N_2. The samples were heated to 1450~1550 ℃

for 3~5 h, and then cooled to room temperature with the furnace. The composite powder was obtained by crushing and grinding the sintered consolidated sample.

2.2. Testing and Characterization

Used X'Pert-Pro-MPDX ray diffraction (XRD) to analyze the primary phases of the composite powder after nitride. Used the Nova 400 Nano electronic microscope (SEM) to observe the microscope of composite powder and energy spectrum analysis of micro-region components (EDS).

3. Results and Discussion

3.1. Phases Composition

Figure 1 shows the XRD pattern of samples with different molar ratios at 1500 ℃ for 4 h in N_2. The main phases of composite powder are Al_2O_3, SiC and β-Sialon, B_4C and Si. And some B_4C reacted to generate BN. As the molar ratio of B_4C and Si decreases from 2:1 to 1:2, the intensity of the diffraction peaks of Al_2O_3, Si and B_4C of the composite powders decreases gradually, and the intensity of diffraction peaks of β-Sialon and SiC increases gradually. The increase of Si content promotes the formation reaction of β-Sialon proceeded. Hence the reaction amount of Al_2O_3 gradually increased, resulting in the relative intensity of its diffraction peak weakening gradually. Due to free carbon in B_4C, Si will react with C. with the increase of Si addition, the amount of SiC will increase. When molar ratio of B_4C, Si is 2: 1, the intensity of diffraction peaks of Si reach the maximum value, which may be due to the low amount of liquid phase of molten Si at this ratio, common wetting and dissolution of other raw materials, and insufficient reaction. While the addition of more Si in A3 and A4 samples leads to the increase of the contact area of reactants in the reactions, and promotes the reaction consumption of Si. The main reason for the low intensity of B_4C diffraction peaks is the formation of liquid phase Si at 1500 ℃. Leads to the increase in contact area and reaction activity between silicon and B_4C particles. Through the dissolution precipitation mechanism [25], the C atoms in B_4C are dissolved in the Si liquid, which promotes the formation of SiC, and then leads to the consumption of B_4C.

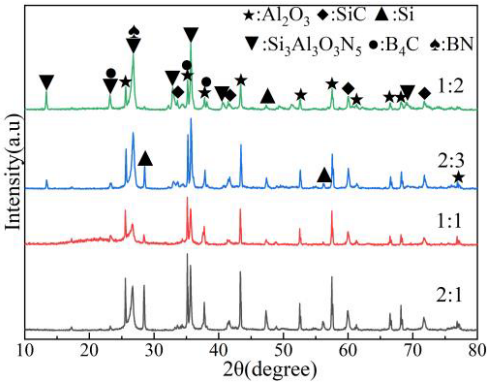

Figure 1. XRD patterns of nitridation samples with different molar ratios at 1500 ℃ for 4 h.

Figure 2 shows the XRD pattern of A3 samples at different nitridation temperatures. The main phases are Al_2O_3, SiC, β-Sialon, B_4C, and AlN. With the increase in sintering temperature, the intensity of the diffraction peaks of Si in the raw material gradually decreases and disappears completely at 1550 ℃. It is speculated that the increase in temperature promotes the reaction consumption of Si, and the reaction is complete at 1550 ℃. At the same time, the diffraction peaks of AlN were detected at 1550 ℃, which may be due to the preferential reaction of some Al vapor with N_2. AlN was formed with the increase of sintering temperature. Insufficient reaction of β-Sialon leads to more residual Al_2O_3. The reaction was sufficient at 1500 ℃, so the intensity of diffraction peaks of Al_2O_3 is low, and the intensity of diffraction peaks of β-Sialon is high. Since silicon reacts completely at 1550 ℃, the relative intensity of the diffraction peak of SiC is the highest.

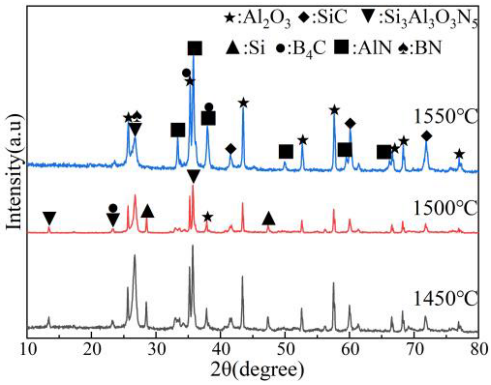

Figure 2. XRD patterns of nitridation of A3 samples at different sintering temperatures for 4 h.

Figure 3 shows the XRD pattern of A3 samples with different soaking times at 1500 ℃. With the extension of soaking time, the intensity of the diffraction peaks of β-Sialon increase gradually and reach the highest intensity at 5 h. At the same time, the diffraction peak of Si can be detected, but its residual is limited. At the same time, the extension of soaking time also promotes the formation of SiC, resulting in higher relative intensity of diffraction peaks. However, too short or too long soaking time will lead to the insufficient reaction of Al_2O_3, which is not conducive to β-Sialon generation.

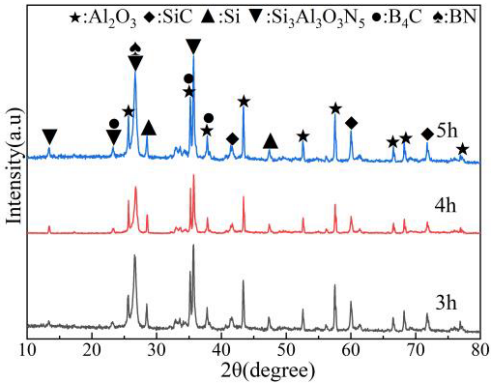

Figure 3. XRD patterns of nitridation of A3 samples with different soaking times at 1500 ℃.

3.2. Micromorphology

Figure 4 is the SEM images of samples with different molar ratios nitrided at 1500 ℃ for 4 h. Figure 4 (a) shows the small-size grains that have not yet been fully developed grow on the large B_4C particles at 1500 ℃. Due to the increase of Si addition, the second phase grains increase significantly, and the grain size increases slightly in figure 4(b). As can be seen in figures 4(c) and (d), due to the further increase of Si addition, the size of small grains increases significantly in the axial direction. A small number of columnar grains were observed in the A3 sample, which is consistent with the typical structure of the β-Sialon phase. But there are still some undeveloped grains. When the molar ratio of B_4C/Si is 1:2, the micro morphology of the sample is similar to the A3 sample. Except that the grains in local areas are coarsened, and a small number of flaky grains appear. It shows that the decrease of the B_4C/Si molar ratio can promote the formation of β-Sialon, and it is consistent with the detection results of the above XRD patterns.

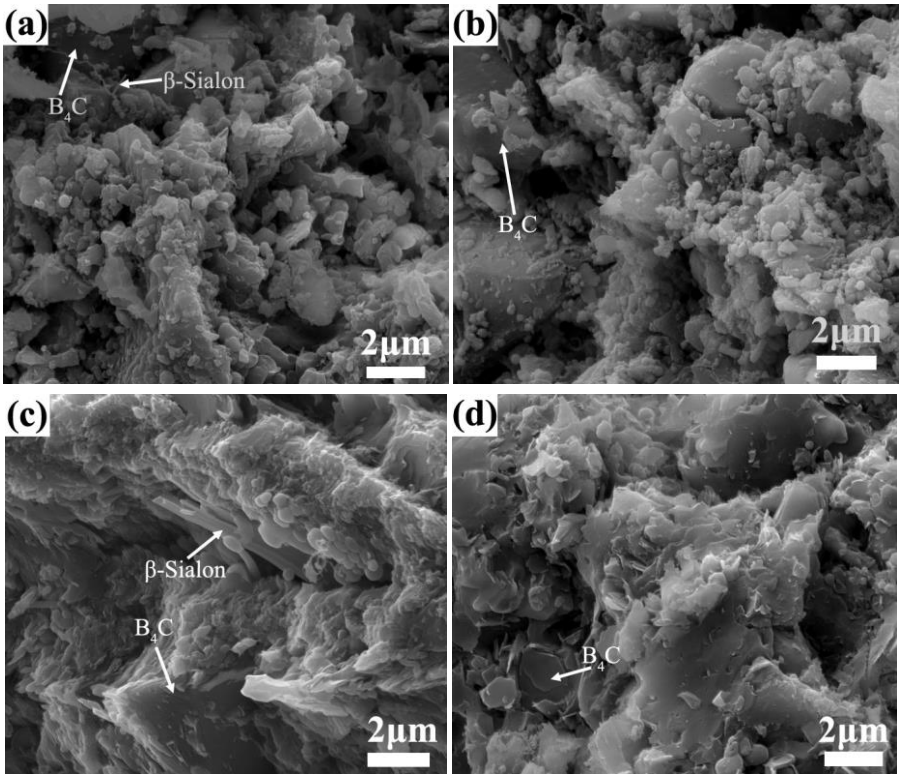

Figure 4. SEM images of samples with different molar ratios after nitridation at 1500 ℃ for 4 h: (a) A1, (b) A2, (c) A3, (d) A4.

Figure 5 shows the SEM images of the A3 sample nitrided and kept for 4 h at 1450~1550 ℃. Figure 5(a) shows with the increase in sintering temperature, the morphology of grains in the sample gradually tends to be regular and neat, growing from the short rod and granular. Figures 5(b) and (c) shows the column and whisker grains. And these columnar grains and whiskers are crisscrossed in the boron carbide

matrix and grow on the surface of large particles. As shown in table 1, columnar grains (point 1) and whiskers (point 2) are accordances with the elemental composition of β-Sialon, SiC, and AlN, due to the effect of residual Al_2O_3, the atomic ratio is different. Due to the aggregation of various substances in the energy spectrum region, it is different from the standard atomic ratio of materials. Combined with the above XRD analysis, it can be inferred that the prismatic particles formed at 1500 ℃ are β-Sialon. The whiskers generated are due to the increase of sintering temperature [26]. Al vapor reacts with N_2 to generate AlN whisker at 1550 ℃, Si vapor reacts with B_4C to generate SiC whisker at 1550 ℃.

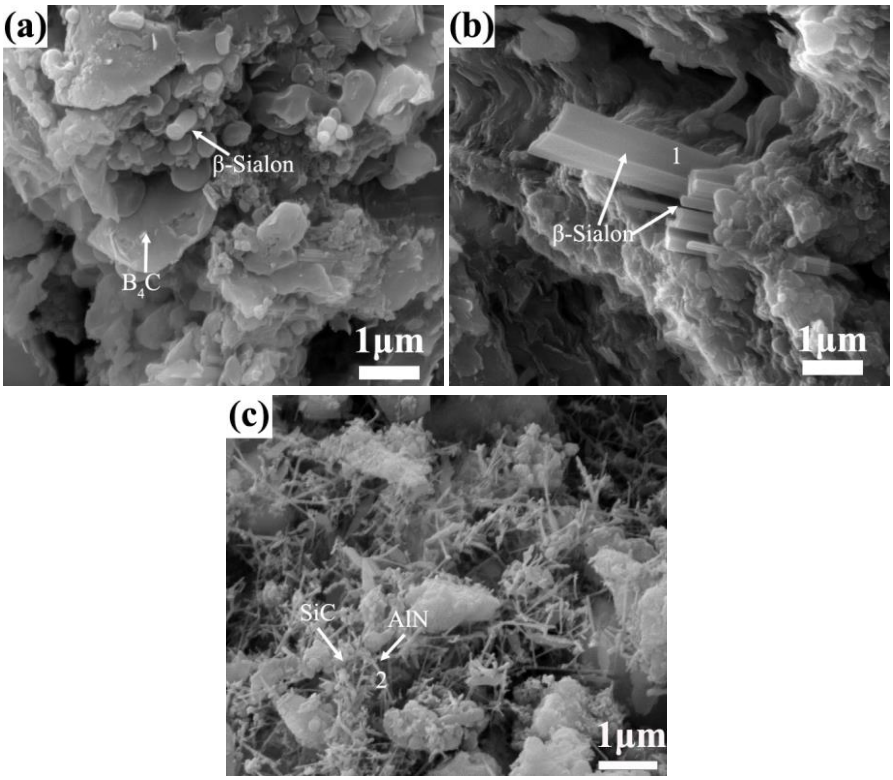

Figure 5. SEM images of the A3 samples after nitridation and soaking for 4 h at different temperatures: (a) 1450 ℃, (b) 1500 ℃, (c) 1550 ℃.

Table 1. Micro area composition/Atomic% of figure 5.

Element	Al	Si	O	N	B	C
1	18.73	9.15	30.15	41.97	–	–
2	10.58	13.69	12.95	19.13	18.72	24.93

Figure 6 shows the SEM images of the A3 sample obtained by soaking for 3 h, 4 h and 5 h respectively at 1500 ℃. With the extension of soaking time, it can significantly promote the radial growth of β-Sialon grains. From the irregular growth in figure 6 (a) to the neat and regular grains in figures 6(b) and (c). The grains growth is incomplete and still in the state of small particles when soaking for 3 h. When soaking for 4 h and

5 h, columnar grains and whiskers arranged neatly are generated, as shown in figure 6 (b) and (c). Extended soaking time for the formation of β-Sialon is obviously promoted. When the soaking time is 5h, SiC grows in whisker and staggered distribution. When the soaking time is 4 h, β-Sialon has a significant content and relatively uniform distribution.

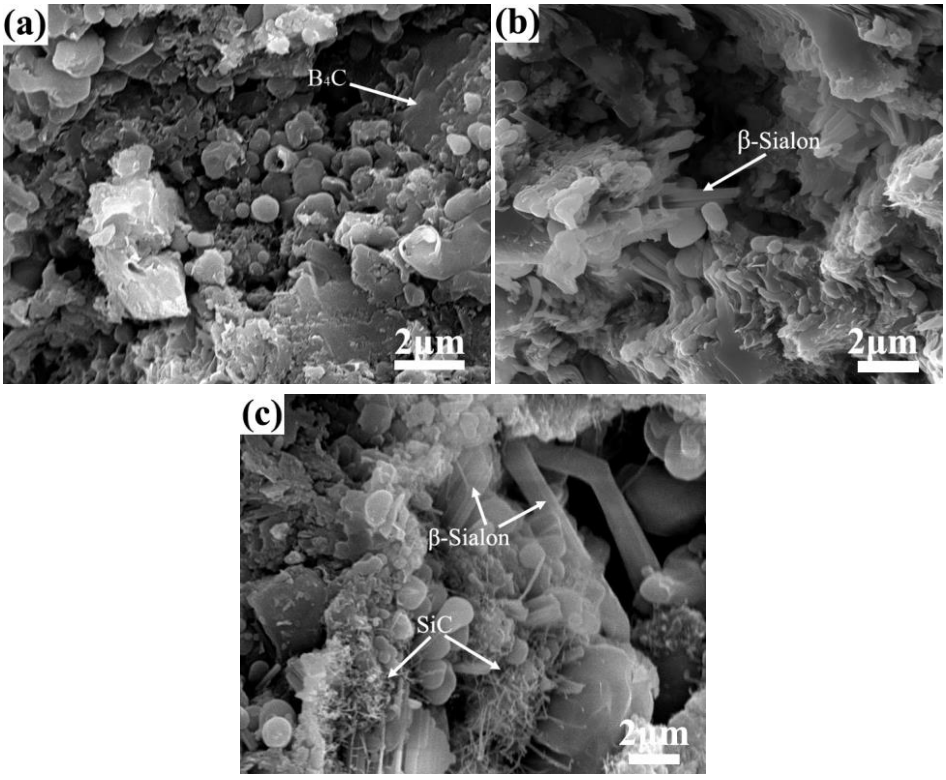

Figure 6. SEM images of nitridation at 1500 ℃ for A3 samples with different holding time: (a) 3 h, (b) 4 h, (c) 5 h.

4. Conclusion

The relatively content of β-Sialon is higher and remaining Si and Al_2O_3 are minor when the molar ratio of B_4C/Si is 2: 3. Excessive Si can cause B_4C to dissolve in Si liquid and cause reaction consumption. It is more full of the form of β-Sialon in the composite powder at 1500 °C for 4 h. The β-Sialon grains grow towards the edge and staggered between B_4C grains in composite powder. Molten Si promotes the dissolution of B_4C and Al_2O_3 in the liquid Si, thus promoting formation of β-Sialon and SiC. Too high nitridation temperature and too long soaking time will lead to volatilization liquid. They are also inhibit the formation of β-Sialon and promotes the formation of SiC and AlN whiskers.

Acknowledgments

This work was supported by the Key Research and Development Project of Hubei Province (Grant No. 2020BAA028), the Science Fund for Creative Research Groups of the National Natural Science Foundation of Hubei Province (Grant No. 2020CFA038) and the National Natural Science Foundation of China (Grant Nos. 51972242, 51774218 and U20A20239).

References

[1] Avcioglu S, Kaya F, Kaya, C. Effect of elemental nano boron on the transformation and morphology of boron carbide (B_4C) powders synthesized from polymeric precursors. Ceram. Int. 2020 Aug; 46(11): 17938-17950.
[2] Jung CH, Lee MJ, Kim CJ. Preparation of carbon-free B_4C powder from B_2O_3 oxide by carbothermal reduction process. Mater. Lett. 2004 Feb; 58(5): 609-614.
[3] Pei LZ, Xiao HN. B_4C/TiB_2 composite powders prepared by carbothermal reduction method. J. Mater. Process. Technol. 2009 Feb; 209(4): 2122-2127.
[4] Lyu XX, Zhao ZY, Sun HL, Jiang XS, Hu CF, Song TF, Luo ZP. Influence of Y_2O_3 contents on sintering and mechanical properties of B_4C-Al_2O_3 multiphase ceramic composites. J. Mater. Res. Technol. 2020 Sept-Oct; 9(5): 11687-11701.
[5] Zhao T,Yu TB, Guan C, Sun JY, Tan XF. Microstructure and friction coefficient of ceramic (TiC, TiN and B_4C) reinforced Ni-based coating by laser cladding. Ceram. Int. 2019 Nov; 45(16): 20824-20836.
[6] Chen HJ, Yang JX, Shuai Q, Li J, Ouyang Q, Zhang S. In-situ doping B_4C nanoparticles in PAN precursors for preparing high modulus PAN-based carbon fibers with boron catalytic graphitization. Compos. Sci. Technol. 2020 Nov; 200: 108455.
[7] Ding DH, Chong XC, Xiao GQ, Lv LH, Lei CK, Luo JY, Zang YF. Combustion synthesis of $B_4C/Al_2O_3/C$ composite powders and their effects on properties of low carbon MgO-C refractories. Ceram. Int. 2019 Sept; 45(13): 16433-16441.
[8] Rahimi A, Baharvandi H. Effect of tungsten carbide nanoparticles on mechanical properties and sinterability of B_4C-WC nanocomposites using pressureless sintering method. Int. J. Refract. Met. Hard Mater. 2017 Aug; 66: 220-225.
[9] Ding J, He WZ, Yu C, Liu ZL, Deng CJ, Zhu HX. Waste biomass derived carbon supported Mo_2C/C composite materials for heavy metal adsorption and hydrogen evolution reaction. Mater. Today Commun. 2022 Jun; 31: 103646.
[10] Hayun S, Dilman H, Dariel MP, Frage N. The effect of aluminum on the microstructure and phase composition of boron carbide infiltrated with silicon. Mater. Chem. Phys. 2009 Dec; 118(2-3): 490-495.
[11] Wang LY, Wang S, Xing PF, Yang MS, Li HQ, Zhuang YX, Du XH. High-performance B_4C-YB_4 composites fabricated with Y_2O_3 additive via hot-pressing sintering. Ceram. Int. 2022 Jun; 48(11): 15647-15656.
[12] Khajehzadeh M, Ehsani N, Baharvandi HR, Abdollahi A, Bahaaddini M, Tamadon A. Thermodynamical evaluation, microstructural characterization and mechanical properties of B4C–TiB2 nanocomposite produced by in-situ reaction of Nano-TiO_2. Ceram. Int. 2020 Dec; 46(17): 26970-26984.
[13] So SM, Choi WH, Kim KH, Park JS, Kim MS, Park J, Lim YS, Kim HS. Mechanical properties of B_4C–SiC composites fabricated by hot-press sintering. Ceram. Int. 2020 May; 46(7): 9575-9581.
[14] Wang Y, Liu Q, Zhang B, Zhang HQ, Jin YC, Zhong ZX, Ye J, Ren YH, Ye F, Wang W. Microstructure and mechanical behaviour of transient liquid phase spark plasma sintered B_4C–SiC–TiB_2 composites from a B_4C–$TiSi_2$ system. Ceram. Int. 2021 Apr; 47(8): 10665-10671.
[15] Du XW, Wang Y, Zhang ZX, Zhang F, Wang WM, Fu ZY. Effects of silicon addition on the microstructure and properties of B_4C–SiC composite prepared with polycarbosilane-coated B_4C powder. Mater. Sci. Eng., A. 2015 Jun; 636: 133-137.
[16] Yavas B, Sahin F, Yucel O, Goller G. Effect of particle size heating rate and CNT addition on densification, microstructure and mechanical properties of B_4C ceramics. Ceram. Int. 2015 Aug; 41(7): 8936-8944.
[17] Liu YY, Li ZQ, Peng YS, Huang YH, Huang ZR, Zhang DK. Effect of sintering temperature and TiB_2 content on the grain size of B_4C-TiB_2 composites. Mater. Today Commun. 2020 Jun; 23: 100875.

[18] Liu ZL, Deng CJ, Yu C, Wang X, Ding J. Zhu HX. Molten salt synthesis and characterization of SiC whiskers containing coating on graphite for application in Al_2O_3-SiC-C castables. J. Alloy. Compd. 2019 Mar; 777: 26-33.

[19] Li W, Wang X, Deng CJ, Yu C, Ding J, Zhu HX. Molten salt synthesis of Cr_3C_2-coated flake graphite and its effect on the physical properties of low-carbon MgO–C refractories. Adv. Powder Technol. 2021 Jul; 32: 2566–2576.

[20] Chen Y, Deng CJ, Wang X, Yu C, Ding J, Zhu HX. Evolution of c-ZrN nanopowders in low-carbon MgO–C refractories and their properties. J. Eur. Ceram. Soc. 2021 Jan; 41(1): 963-977.

[21] Li W, Deng CJ, Chen Y, Wang X, Yu C, Ding J, Zhu HX. Application of Cr_3C_2/C composite powders synthesized via molten-salt method in low-carbon MgO–C refractories. Ceram. Int. 2022 Jun; 48(11): 15227-15235.

[22] Jung SG, Seong WK, Lee NH, Kang WN. Effect of columnar grain boundaries on flux pinning in MgB_2 films. Phys. C. 2011 Nov; 471(21-22): 798-800.

[23] Biswas M, Bandyopadhyay S, Bhattacharya D. Synthesis of pure 15R–SiAlON polytype phase & its crystal structure under carbothermal-reduction-nitridation. Mater. Chem. Phys. 2020 Mar; 243: 122617.

[24] Chen Y, Deng CJ, Wang X, Ding J, Yu C, Zhu HX. Effect of Si powder-supported catalyst on the microstructure and properties of Si_3N_4-MgO-C refractories. Constr. Build. Mater. 2020 Apr; 240: 117964.

[25] Tian T, He QL, Liu C, Wang AY, Hu LX, Guo WC, Wang WM, Wang H, Zou J, Fu ZY. The effect of B and Ti–Al intermetallics additions on the microstructure and mechanical properties of hot-pressed B_4C. Ceram. Int. 2022 Jun; 48(11): 16054-16062.

[26] Zhao XQ, Zou J, Ji W, Wang AY, He QL, Xiong ZG, Wang WM, Fu ZY. Processing and mechanical properties of B_4C-SiC_w ceramics densified by spark plasma sintering. J. Eur. Ceram. Soc. 2022 May; 42(5): 2004-2014.